The Dwarf Novae of Shortest Period [1]

John R. Thorstensen
Department of Physics and Astronomy
6127 Wilder Laboratory, Dartmouth College
Hanover, NH 03755-3528
electronic mail: `thorstensen@dartmouth.edu`

Joseph O. Patterson, Jonathan Kemp
Department of Astronomy, Columbia University
538 West 120th Street, New York, NY 10027
electronic mail: `jop@astro.columbia.edu`

Stéphane Vennes
Astrophysical Theory Centre
Australian National University, ACT0200, Australia
electronic mail: `vennes@wintermute.anu.edu.au`

ABSTRACT

We present observations of the dwarf novae GW Lib, V844 Her, and DI UMa. Radial velocities of Hα yield orbital periods of 0.05332 ± 0.00002 d (= 76.78 m) for GW Lib and and 0.054643 ± 0.000007 d (= 78.69 m) for V844 Her. Recently, the orbital period of DI UMa was found to be only 0.054564 ± 0.000002 d (= 78.57 m) by Fried et al. (1999), so these are the three shortest orbital periods among dwarf novae with normal-abundance secondaries.

GW Lib has attracted attention as a cataclysmic binary showing apparent ZZ Ceti-type pulsations of the white dwarf primary. Its spectrum shows sharp Balmer emission flanked by strong, broad Balmer absorption, indicating a dominant contribution by white-dwarf light. Analysis of the Balmer absorption profiles is complicated by the unknown residual accretion luminosity and lack of coverage of the high Balmer lines. Our best-fit model atmospheres are marginally hotter than the ZZ Ceti instability strip, in rough agreement with recent ultraviolet results from HST. The spectrum and outburst behavior of GW Lib make it a near twin of WZ Sge, and we estimate it to have a quiescent $M_V \sim 12$. Comparison with archival data reveals proper motion of 65 ± 12 mas yr^{-1}.

The mean spectrum of V844 Her is typical of SU UMa dwarf novae. We detected superhumps in the 1997 May superoutburst with $P_{\rm sh} = 0.05597 \pm 0.00005$ d. The spectrum of DI UMa appears normal for a dwarf nova near minimum light.

These three dwarf novae have nearly identical short periods but completely dissimilar outburst characteristics. We discuss possible implications.

Subject headings: stars – individual; stars – binary; stars – variable.

1. Introduction

Cataclysmic variable stars are close binary systems in which mass is transferred from a low-mass

[1] Based in part on observations obtained at the Michigan-Dartmouth-MIT Observatory.

secondary onto a white dwarf; Warner (1995) has written an excellent monograph on cataclysmics. In the dwarf nova subclass, the transferred matter is thought to accumulate in an accretion disk until a critical density is reached, whereupon the transfer of matter through the disk dramatically increases, causing a brightening of the star. The outbursts of dwarf novae range widely in amplitude and frequency, with the less-frequently outbursting systems tending to have the greatest amplitudes (the Kukarkin-Parenago relation).

The orbital periods $P_{\rm orb}$ of dwarf novae range from $\sim$ 12 hours down to about 75 minutes, near the theoretical minimum period for a hydrogen-rich donor star (Rappaport, Joss, & Webbink 1982). (We do not here consider systems with helium donor stars, which can reach much shorter periods.) Dwarf novae with $P_{\rm orb}$ less than about 3 h (effectively, those shortward of the 2-3 h period 'gap') show occasional large-amplitude, long-duration outbursts, called superoutbursts, which are accompanied by photometric oscillations, called superhumps, which have periods $P_{\rm sh}$ a few percent *longer* than $P_{\rm orb}$. Superoutbursters are classified as SU UMa stars, after their prototype. But SU UMa stars show a wide range of intervals between outbursts, from about 4 days for ER UMa and its brethren (Jablonski & Cieslinski 1992; Patterson et al. 1995; Robertson, Honeycutt, & Turner 1995; Misselt & Shafter 1995; Thorstensen et al. 1997), to several decades for WZ Sge and similar stars (O'Donoghue et al. 1991; Patterson et al. 1996, 1998; Kato & Kunjaya 1995).

Here we report extensive observations of the dwarf novae GW Lib and V844 Her, which prove to have very short orbital periods. We also present a spectrum of DI UMa, another very short period system. In spite of their similar orbital periods, these three systems have quite different outburst characteristics.

Section 2 of this paper describes observational protocols and the analysis which produced orbital periods for GW Lib and V844 Her. Sections 3, 4, and 5 contain more detailed discussions of GW Lib, V844 Her, and DI UMa respectively. Finally, Section 6 contrasts the three systems and discusses implications for cataclsymic binary evolution.

2. Observations

Our spectroscopy is from the 2.4 m Hiltner telescope at MDM Observatory. The modular spectrograph and a 2048^2 CCD detector gave spectra covering 4300 – 7500 Å at 2 Å pixel^{-1}, and a 1 arcsec slit gave 3.5 Å resolution over most of the range. We observed flux standards when appropriate, took comparison lamps frequently as the telescope tracked, and reduced the data using standard procedures in IRAF. A few spectra were adjusted slightly in velocity when checks of the λ5577 night-sky line revealed that a comparison lamp exposure had gone awry. From these checks we estimate our velocity scale to be correct to within ~ 10 km s^{-1} and rather more stable than this. The flux scale suffers from occasional clouds, uncalibrated losses at the spectrograph slit, and a poorly-understood instrumental problem which causes inconsistent continuum shapes among the standard stars. The spectra shown here are averages of many, which appears to have ameliorated these problems. Figs. 1 and 2 show averaged spectra of all the objects, and Table 1 gives quantitative measures of the spectra.

For GW Lib and V844 Her, our spectra were extensive enough for us to derive orbital periods. We measured velocities of the Hα emission using convolution techniques (Schneider & Young 1980), and searched for periods among the resulting time series (Fig. 3) using the sinusoidal fit method described by Thorstensen et al. (1996). To asses the reliability of alias choices we used the Monte Carlo test of Thorstensen & Freed (1985). Table 2 (available in full in the electronic version of this paper) lists the radial velocities, Table 3 gives sinusoidal fits to the velocities at the preferred periods of the form

$$v(t) = \gamma + K \sin[2\pi(t - T_0)/P],$$

and Fig. 4 shows the velocities folded at the best periods, with the fits superposed. In Table 3, σ is the uncertainty of a single velocity derived from the goodness of fit. Because the emission lines may not reflect the motion of either star accurately, we caution against using γ or K for dynamics. However, experience suggests that the spectroscopic P should be a reliable measure of $P_{\rm orb}$.

Our photometric data are more various. We obtained time-series photometry of the outburst of V844 Her using the Center for Backyard Astrophysics network of photometrists (e.g., Patterson et al. 1998). In addition, on 2000 Jan. 11 UT we obtained $UBVRI$ images of GW Lib with the Hiltner 2.4 m and the central 1024^2 pixels of a SITe 2048^2 CCD, at a scale of 0.275 arcsec pixel^{-1}. These were calibrated with observations of Landolt (1992) standard stars.

3. GW Lib

GW Lib was discovered in 1983 as a 9th magnitude novalike object (González & Maza 1983). After the object faded to $V \sim 16$, Duerbeck & Seitter (1987) found a strong blue continuum with relatively sharp Balmer emission lines. Duerbeck (1987) lists its classification as uncertain between nova or dwarf nova. Ringwald, Naylor, & Mukai (1996) also show a spectrum, note its similarity to WZ Sge, and classify GW Lib as a dwarf nova. The outburst recurrence time is likely to be very long (≥ 10 yr), though outbursts could have gone undetected given the star's low ecliptic latitude ($-6^\circ.4$).

van Zyl et al. (2002) report extensive time-series photometry of GW Lib in 1997, 1998, and 2001, and found dominant oscillations at periods near 650, 370, and 230 s. The pulsation spectrum is unstable, with many signals closely spaced in frequency. They interpret these signals as arising from non-radial pulsations of the white dwarf, making it the only such pulsator also known to be accreting. A report of their early results prompted us to observe the star in 1999 June.

Szkody, Desai, & Hoard (2000) report spectroscopy of GW Lib, from which they derived an orbital period of 79.4 ± 0.3 minutes and found the signature of a white dwarf photosphere in the mean spectrum. Our results described below are in broad agreement, but we do find a significantly shorter orbital period of 76.79 ± 0.02 min. Many of our observations occurred on adjacent nights, allowing cycles to be counted from night to night, but their three nights were separated too widely in time to allow this. Thus the present determination supersedes that of Szkody, Desai, & Hoard (2000). Szkody et al. (2002) also obtained an HST spectrum in 2002 January which indicates a white-dwarf temperature of 14,700 kelvin; our less precise measure (see below) is in satisfactory agreement with this determination.

Intriguingly, Woudt & Warner (2002) detected a 2.09-h photometric modulation in observations obtained 2001 May (but not in observations obtained at other times). They note that this periodicity has no particular relationship to the orbital period, and that its cause is unknown.

3.1. Spectroscopy

Because of GW Lib's southerly declination, we pushed the observations to airmasses as large as 4.6 to obtain the largest possible range of hour angle, and hence the greatest discrimination between daily cycle-count aliases. The resulting data set spans 5.5 h, and includes 88 exposures of 300 s each. In the mean spectrum (Fig. 1) the continuum at $\lambda 5500$ corresponds to $V \sim 17.4$; because an unknown fraction of the light is lost at the slit, this is in fair agreement with the magnitudes derived from the CCD photometry, namely $V = 17.01, B - V = 0.12, U - B = -0.50$, and $V - I_{KC} = 0.12$. The strong blue continuum and Balmer absorption wings suggest that the bulk of the light arises in a white dwarf photosphere. The Balmer emission lines are unusually narrow, with Gaussian fits giving ~ 10 Å FWHM (full width half maximum). Weak HeI emission is visible at $\lambda\lambda$ 5876, 6678, and 7027. An emission feature near λ 5169 is present, which is usually attributed to FeII, and the Na D lines appear weakly in emission. All other features are artifacts; they include incompletely subtracted night sky lines at $\lambda\lambda$ 5577 and 6300, and a telluric absorption band at λ 6870 which did not divide out completely.

The convolution function used for the velocities was optimized for 10 Å FWHM, so our velocities pertain to the narrow line core. The periodogram (Fig. 3) indicates an orbital frequency near 18.75 cycles d^{-1}, and the Monte Carlo test shows that the choice of daily cycle count is secure at > 99 per cent confidence. The orbital period – 76.79 ± 0.02 min – is the shortest known for dwarf nova accreting from companions with normal hydrogen abundances (the secondary stars in shorter-period objects such as RX2329+06 are probably enriched in helium; Thorstensen et al. 2002).

3.2. Binary Inclination, Accretion Rate, Distance, and Proper Motion

The long outburst interval, short orbital period, and spectral appearance of GW Lib make it an excellent match for WZ Sge. In Fig. 1 we present a spectrum of WZ Sge for comparison – they appear very similar, except the emission lines of GW Lib are much narrower.

The narrowness of the emission lines suggests a low binary inclination. WZ Sge has $i \sim 77°$ (Spruit & Rutten 1998), and the emission lines in our spectrum of WZ Sge are about five times wider than those in GW Lib. Attributing the difference entirely to inclination leads to an estimate of $i \approx 11°$. The emission in WZ Sge has a strong S-wave component; we do not resolve this component in GW Lib (indeed, we don't see any clear substructure in the emission lines), but an S-wave contribution may be dominating the apparent motion of the line.

Apparently, no accurate photometry was obtained during GW Lib's only known outburst, but the photographic magnitude at discovery was estimated as 9.0. Since $B - V \approx 0.$ for dwarf novae in outburst, we take the outburst V magnitude to be near 9. Warner (1995) presents a standard-candle relationship for dwarf novae in outburst, which predicts an $M_V = +5.4$ at this $P_{\rm orb}$. Superoutbursts tend to be about 1 mag brighter than this, so we estimate $M_V = +4.5$. Warner's relation is reckoned at $i = 56°$, but GW Lib is evidently more face-on than this, making it about 1 magnitude brighter than at the canonical inclination, or $M_V = +3.5$. This would put GW Lib at only ~ 125 pc distance. Our quiescent $V = 17.0$ then implies $M_V \approx +11.5$.

Because of the short distance indicated by the above arguments, we searched for a proper motion. The Digitized Sky Survey has two epochs available, 1976.3 and 1991.3. GW Lib was also imaged in the original Palomar Observatory Sky Survey (epoch 1955.4 for this field), and Dr. David Monet of USNO kindly provided us with coordinates from this survey measured with the USNO Plate Measuring Machine. We use our I-band 2.4m CCD image for the final epoch (2000.02). The CCD image gave the best internal precision, so we fit centroids from this image to the USNO A2.0 catalog to derive refined nominal standard coordinates for 99 field stars, and then transformed coordinates from the other images onto this system using 6-constant plate model fits. GW Lib showed a significant proper motion $\mu = 66 \pm 12$ mas yr^{-1} in position angle 296 ± 10 degrees. This corroborates a short distance; its transverse velocity would be 39 km s^{-1} at 110 pc. The celestial coordinates of GW Lib for epoch and equinox 2000 refererred to the USNO A2.0 system (nominally ICRS) are $\alpha = 15^{\rm h}\ 19^{\rm m}\ 55^{\rm s}.33$ and $\delta = -25°\ 00'\ 24''.7$.

3.3. Line Profile Analysis

We estimated the white dwarf's atmospheric parameters by fitting the Balmer line profiles to a grid of synthetic white-dwarf spectra spanning $T_{\rm eff}$ from 10000 to 84000 kelvin and $\log g$ from 7.0 to 9.0, with log(He/H) = -9. These were computed using a new version of the Mihalas, Auer, & Heasley (1975) computer code modified to include convection within the existing numerical treatment. Potential convective instability of each depth layer was tested against the standard Schwarzschild criterion and the convective flux was computed using the mixing length formalism (Mihalas 1978). We adopted convective parameters appropriate for ZZ Ceti white dwarfs following the analysis of Bergeron et al. (1995), namely the ML2 parameters with the mixing length over pressure scale height ratio α adjusted to 0.6. Neutral hydrogen b-b, b-f, and f-f opacities as well as b-f and f-f opacities of the negative hydrogen ion are included in the calculation. The model atmospheres are converged until the total flux is constant to at least one part in 10^6. Detailed Stark-broadened synthetic line profiles are computed based on the converged models.

Fig. 5 shows the best fit to the Hα and Hβ line profiles. The central emission is excluded from the fit ($\pm 50\mathring{A}$). A general search between T_{eff} = 10,000 K and 30,000 K reveals a best solution at $T_{eff} = 24,000$ and log $g = 8.76$. This solution is totally incompatible with the optical spectral energy distribution which imposes a much cooler temperature. Restricting the fit to the range of temperature between 10,000 and 14,000 K reveals a solution close to 13,000 K. A slightly different solution is obtained when excluding ±40Å from the Hα core, and ±30 Å from Hβ. A comparison of the two solutions underlines systematic effects due to the incompleteness of the data set. Adding possible continuum disk contamination to the synthetic spectra in the form of a contribution corresponding to 5% and above of the observed flux at 5500Å, eliminates all solutions below 16,000 kelvin, so the disk contamination appears to be small.

The best-fit parameters (T_{eff} = 13220K, log$g = 7.4$) are above the ZZ Ceti instability strip but the 90% confidence contour extends within the range ascribed to the pulsating class of DA white dwarfs by Bergeron et al. (1995), using the ML2 $\alpha = 0.6$ formalism. The results of the present analysis are uncertain, because (1) systematic effects such as disk contamination are not well ascertained and (2) the quality of the line profile fit is not satisfactory and is based on only two lines. As noted earlier, Szkody et al. (2002) find a temperature of 14,700 K for the white dwarf based on an HST UV spectrum; our result is consistent with theirs, but is likely to be less accurate for the reasons noted above.

4. V844 Herculis

V844 Herculis is a dwarf nova discovered by Antitpin (1996) in a search for variable stars in a photographic survey with the 40 cm Crimean astrograph. On 419 plates in the interval 1960-1994, Antipin found variations in the range B=12.5-17.5, with the best-observed outburst lasting 12-18 days. This announcement captured the attention of variable-star observers, and the star has now become frequently monitored by visual observers. Long outbursts were seen in May 1997 and December 1998, and the outburst of October 1996 was probably also long. The interval between these long outbursts is not securely known, but is probably about 280 days.

4.1. The May 1997 Outburst

News of the May 1997 outburst drove the CBA network into action. Starting with the third night of outburst, we obtained photometric coverage on 21 of 37 nights, following the star all the way down to quiescence. The photometry log is given in Table 4.

The eruption timescale (15 d bright, followed by rapid return to quiescence in 1-2 d) is typical of superoutbursts in SU UMa stars. Even more characteristic are the photometric waves (superhumps) prominent throughout the eruption. Fig. 6 (upper panel) shows the superhumps in one long night of coverage. These establish the star's membership in the SU UMa class of dwarf novae.

We calculated the mean superhump amplitude and time of maximum light for each night of observation. These measurements are given in the final columns of Table 4. The amplitude spectrum of the 10-day superoutburst light curve (JD 2450592-602) is shown in the lower panel of Fig. 6, indicating a powerful signal at 17.87 ± 0.02 cycle d^{-1} and its first harmonic. A signal is seen near 71.88 cycle d^{-1} also. Since we know the orbital frequency to be $\omega = 18.300$ cycle d^{-1} (see below), we interpret 17.87 cycle d^{-1} as the basic superhump frequency, the $\omega - \Omega$ lower precessional sideband of the orbital frequency. Then the 35.75 cycle d^{-1} signal is the first harmonic, at $2\omega - 2\Omega$. The identification of the 71.88 cycle d^{-1} signal is less clear, but it could be the $4\omega - 3\Omega$ component (in general, superhumps come with $n\omega - m\Omega$ components, where m and n are any small integers and $m \leq n$; Skillman et al. 1999). The superhump *changes* measurably in frequency and waveform during the 10-day interval, so precise identification of higher components is somewhat ambiguous.

4.2. Spectroscopy

Our spectra are from 1997 June and July, after the star had returned to quiescence. The observations, comprising 158 300-s exposures, span 18 d of elapsed time and 7.06 h of hour angle. The mean spectrum (Fig. 2) is normal for a dwarf nova; in particular, the hydrogen and helium lines appear similar to other dwarf novae of longer period, emphasizing that the accreted material must come from the usual hydrogen-envelope secondary despite the short orbital period. The emission lines are double-peaked; in Hα and Hβ, the peaks are separated by ±400 km s^{-1} and at the half-intensity points the lines extend to ±900 km s^{-1}. The continuum level implies $V \sim 17.9$, with an uncertainty of a few tenths from unknown light losses at the spectrograph slit. The Hα emission velocities (Table 2) were measured using the derivative of a Gaussian as the convolution function; this was optimized for a 40 Å line width, a little wider than the 36 Å observed width of Hα, in order to emphasize the wings of the line profile. We found that the velocity amplitude was strongly affected by the algorithm used, reinforcing the usual cautions about using CV emission lines for dynamical mass estimates. However, the period (Table 3) is determined without ambiguity.

5. DI Ursae Majoris

DI UMa (Fried et al. 1999; Kato, Nogami, & Baba 1996) has superoutbursts recurring on a timescale of 30 to 45 d. This places it among the most frequently superoutbursting SU UMa stars, a group loosely referred to as the ER UMa stars. We did not accumulate sufficient spectra to find an independent orbital period; photometry at quiescence Fried et al. (1999) yields a modulation at 0.054564 ± 0.000001 d ($= 78.57$ min), which is presumably the orbital period. Fig. 2 shows the mean spectrum, and Table 1 lists the spectral features. The normality of the spectrum suggests that the abundances in the accreting material are normal, which in turn suggests that the secondary is not enriched in helium.

6. Discussion

In Table 5 we list the seven dwarf novae (or dwarf-nova candidates) with the shortest well-established orbital periods. Two of the systems have periods shorter than GW Lib. V485 Cen has a dramatically short 59-min period. Augustein et al. (1996) explain this by invoking a low hydrogen abundance for the secondary, so it may not belong among the more usual hydrogen accretors. Support for this idea comes from the apparently related system RX2329+06, which has a K-type secondary at $P_{\mathrm{orb}} = 64$ min, a period at which a CV secondary with normal hydrogen abundance would be be much cooler. Thorstensen et al. (2002) show that a helium-enriched secondary matches the observations, and propose that mass transfer began near the end of core hydrogen burning. Another system, RX2353−38, resembles a dwarf nova spectroscopically, and it probably is one, but it has never been observed to erupt. Thus the stars studied here have the three shortest periods among well-established, hydrogen-accreting dwarf novae.

In the most straightforward scenarios for CV evolution (see King (1988) for a review), the properties of dwarf novae are regulated by the accretion rate, which is dependent on the mass of the secondary, which depends on orbital period. Thus the outburst properties should depend in a simple way on P_{orb}. In particular, stars of the shortest orbital period should have very rare outbursts, like the well-studied prototype WZ Sge.

The truth appears to be much more complex. One of these stars, GW Lib, is indeed an excellent match to WZ Sge: intrinsically very faint, with a recurrence period probably exceeding 10 years. Yet DI UMa is a rather bright star (at the distance estimated by Fried et al. (1999) it would have $M_V = +8.4$ at minimum), and one of the most frantic dwarf novae in the sky, erupting at least 100 times more frequently. And V844 Her is an intermediate case, but unusual in never having shown any normal outbursts (despite the modest interval of ~ 280 d between superoutbursts). This is more or less the full range of activity (and brightness) displayed by dwarf novae. Yet it occurs in three binaries with orbital periods equal to within 2 minutes.

Why this should be so remains a mystery. Perhaps there are cycles in the mass-transfer rate over timescales long compared to the historical record, but short compared to the evolutionary timescale (King et al 1996; Wu, Wickramasinghe, & Warner 1995). Also, in the most common picture of evolution at short period, the angular-momentum loss is thought to be dominated by gravitational radiation, leading to a convergence of evolution among different systems and a universal value for the minimum period. But if another, more idiosyncratic angular momentum loss mechanism persists — magnetic braking is an obvious candidate — the minimum period may not be as clearly defined, and the observed diversity of stars near the minimum may be easier to understand. Indeed, King et al (1996) find that mass-transfer cycles among short-period systems are damped out unless there is some small consequential angular momentum loss (that is, an angular momentum loss mechanism for which $\dot{J}$ increases modestly with $\dot{M}$). Another line of evidence also suggests an extra channel for angular momentum loss. Patterson (1998) notes the apparent discrepancy between the large number of short-period and 'post-bounce' systems predicted by theory, and the much smaller number of such systems which have actually been observed; a second angular momentum loss mechanism which destroys short-period systems would help ameliorate that discrepancy, as well.

Acknowledgments. We thank the NSF for support through grant AST 9987334, and the MDM staff for their support. SV is a QEII fellow of the Australian Research Council.

REFERENCES

Abbott, T. M. C., Fleming, T. A., & Pasquini, L. 1997, A&A, 318, 134

Antipin, S. V., 1996, IBVS, No. 4360

Augusteijn, T., van der Hooft, F., de Jong, J.A., and van Paradijs, J. 1996, A&A, 311, 889.

Augusteijn, T. and Wisotzki, L., 1997, A&A, 324, L57

Bergeron, P., Wesemael, F., Lamontagne, R., Fontaine, G., Saffer, R. A., & Allard, N. F. 1995, ApJ, 449, 258

Duerbeck, H. W. 1987, *A Reference Catalog and Atlas of Galactic Novae*, D. Reidel: Dordrecht, Boston.

Duerbeck, H. W., and Seitter, W. C., Ap&SS131, 467

Duerbeck, H. W., and Mennickent, R. E. 1998, IBVS, No. 4637

Fried, R., Kemp, J., Patterson, J., Skillman, D. R., Retter, A., Leibowitz, E., and Pavlenko, E. 1999, PASP, 111, 1275

González, L. E., & Maza, J. 1983, IAUC No. 3854

Jablonski, F. J., & Cieslinski, D. 1992, å, 259, 198

Kato, T., & Kunjaya, C., 1995, PASJ, 47, 163

Kato, T., Nogami, D., and Baba, H. 1996, PASJ, 48, L93

King, A. R., 1988, QJRAS, 29, 1

King, A. R., Frank, J., Kolb, U., and Ritter, H. 1996, ApJ, 467, 761

Landolt, A. U. 1992, AJ, 104, 340

Mihalas, D. 1978, Stellar Atmospheres (San Francisco:Freeman)

Mihalas, D., Auer, L. H., & Heasley, J. N., 1975, NCAR Technical Note STR-104

Misselt, K. A., & Shafter, A. W. 1995, AJ, 109, 1757

O'Donoghue, D., Chen, A., Marang, F., Mittaz, J. P. D., Winkler, H., and Warner, B. 1991, MNRAS, 250, 363

Olech, A. 1997, Acta Astr, 47, 281

Patterson, J., Jablonski, F., Koen, C., O'Donoghue, D., & Skillman, D. R. 1995, PASP, 107, 1183

Patterson, J., Augusteijn, T., Harvey, D. A., Skillman, D. R., Abbott, T. M. C., and Thorstensen, J. 1996, PASP, 108, 748

Patterson, J. 1998, PASP, 110, 1132

Patterson, J., Kemp, J., Skillman, D. R., Harvey, D. A., Shafter, A. W., Vanmunster, T., Jensen, L., Fried, R., Kiyota, S., Thorstensen, J. R., and Taylor, C. J. 1998, PASP, 110, 1290

Skillman, D. R., Krajci, T., Beshore, E., Patterson, J., Kemp, J., Starkey, D., Oksanen, A., Vanmunster, T., Martin, B., & Rea, R. 2002, PASP, in press.

Rappaport, S., Joss, P. C., Webbink, R. F., 1982, ApJ, 254, 616

Ringwald, F. A., Naylor, T., and Mukai, K. 1996, MNRAS, 281, 192

Robertson, J. W., Honeycutt, R. K., & Turner, G. W. 1995, PASP, 107, 443

Schneider, D. and Young, P. 1980, ApJ, 238, 946

Spruit, H. C., & Rutten, R. G. M. 1998, MNRAS, 299, 768

Szkody, P., Desai, V. & Hoard, D. W. 2000, AJ, 119, 365

Szkody, P., Gänsicke, B., Sion, E. M., & Howell, S. 2002, in preparation.

Thorstensen, J. R. and Freed, I. B. 1985, AJ, 90, 2082

Thorstensen, J. R., Patterson, J., Shambrook, A., and Thomas, G. 1996, PASP 108, 73

Thorstensen, J. R., Taylor, C. J., Becker, C. M., and Remillard, R. 1997, PASP, 109, 447

Thorstensen, J. R., Fenton, W. H., Patterson, J. O., Kemp, J., Krajci, T., & Baraffe, I. 2002, ApJ, 567, L49

van Zyl, L., et al. 2002, MNRAS, submitted.

Warner, B. 1995, Cataclysmic Variables (Cambridge University Press)

Woudt, P. A., & Warner, B. 2002, Ap. Sp. Sci., in press.

Wu, K., Wickramasinghe, D. T., & Warner, B. 1995, Pub. Astron. Soc. Australia, 12, 60

AAS LaTeX macros v5.0.

Table 1
Spectral Features

Star	Feature	E.W.[a] (Å)	Flux[b] (10^{-16} erg cm^{-2} s^{1})
GW Lib	Hβ (emission)	12	40
	FeII λ5169	1.3	6
	HeI λ5876	1.1	4
	Na D (emission)	1.3	4
	Hα (emission)	52	120
	HeI λ6678	1.2	3
V844 Her	Hγ	40	160
	HeI λ4471	7	30
	Hβ	54	180
	HeI λ5015	5	16
	HeI λ5876	19	44
	Hα	98	200
	HeI λ6678	9.5	20
DI UMa	Hγ	20	60:
	Hβ	32	90
	HeI λ4921	2.5:	7:
	HeI λ5015	8.3	27
	HeI λ5876	10	22
	Hα	42	80

[a]Emission equivalent widths are counted as positive.

[b]Absolute line fluxes are uncertain by a factor of about 2, but relative fluxes of strong lines are estimated accurate to ~ 10 per cent.

Table 2
Hα Radial Velocities

HJD[a]	V (km s^{-1})	HJD[a]	V (km s^{-1})	HJD[a]	V (km s^{-1})	HJD[a]	V (km s^{-1})
			V844 Her:				
623.6793	−87	623.8655	137	624.7498	−6	627.8050	51
623.6834	−80	623.8697	61	624.7539	−106	627.8091	46
623.6876	−141	623.8738	69	624.7580	−42	627.8131	54
623.6917	−41	623.8779	10	624.7620	−62	627.8191	−78
623.6958	−29	623.8821	−52	624.7661	−152	627.8232	−136
623.7000	84	623.8862	−48	624.7701	−107	627.8272	−186
623.7041	−112	623.8903	−89	624.7742	−149	627.8313	−42
623.7082	63	623.8945	−149	624.9159	−3	627.8353	−47
623.7149	−37	623.9052	−84	624.9200	−146	627.8394	−31
623.7191	−69	623.9093	−8	624.9240	−87	627.8434	0
623.7232	−132	623.9135	−10	624.9281	−169	631.8717	−174
623.7273	−213	623.9176	65	624.9322	−174	631.8758	−102
623.7315	−182	623.9217	48	624.9362	−175	631.8798	−80
623.7356	−84	623.9259	17	624.9403	−56	631.8839	9
623.7397	−23	623.9300	5	624.9444	−25	631.8879	−29
623.7439	−50	623.9341	−61	624.9504	−25	631.8920	63
623.7509	−68	623.9411	−89	624.9544	−70	631.8961	−6
623.7550	65	623.9452	−168	624.9585	80	631.9001	56
623.7591	48	623.9494	−232	624.9625	31	631.9068	54
623.7633	104	623.9535	−196	624.9666	95	631.9149	−27
623.7674	−60	623.9576	−52	625.7567	−144	631.9189	−97
623.7716	−111	623.9618	5	625.7607	−108	631.9230	−130
623.7757	−78	623.9659	34	625.7648	−90	631.9271	−147
623.7798	−152	624.6732	−33	625.7689	−33	631.9311	−67
623.7919	−116	624.6773	49	625.7729	16	631.9352	−17
623.7961	−55	624.6814	−11	625.7770	100	641.7186	−85
623.8002	15	624.6854	41	625.7811	9	641.7227	9
623.8043	25	624.6895	22	625.7851	−25	641.7267	32
623.8084	44	624.6935	97	625.7916	−12	641.7308	35
623.8126	37	624.6981	−33	625.7957	−119	641.7348	74
623.8167	99	624.7021	−73	625.7997	−66	641.7389	8
623.8208	76	624.7100	−54	625.8038	−151	641.7457	44
623.8289	−75	624.7141	−137	625.8078	−84	641.7497	−62
623.8330	−139	624.7182	−61	625.8119	−157	641.7538	−59
623.8371	−157	624.7222	−54	625.8160	−73	641.7579	−108
623.8413	−136	624.7263	−30	625.8200	−44	641.7619	−191
623.8454	−108	624.7303	−2	627.7888	24	641.7660	−100

Table 2—*Continued*

HJD[a]	V (km s^{-1})	HJD[a]	V (km s^{-1})	HJD[a]	V (km s^{-1})	HJD[a]	V (km s^{-1})
623.8495	−58	624.7344	114	627.7928	−7	641.7723	−181
623.8537	41	624.7385	−7	627.7969	160	641.7775	−39
623.8578	−31	624.7458	29	627.8009	76	641.7815	156
			GW Lib:				
1333.7665	−61	1339.8674	−4	1340.8206	−10	1341.7841	37
1333.7705	−52	1339.8714	15	1340.8247	−1	1341.7992	−7
1333.7746	−31	1340.6566	7	1341.6564	−45	1341.8033	−7
1333.7787	−28	1340.6607	−10	1341.6605	−57	1341.8073	−50
1333.7828	35	1340.6647	5	1341.6645	−35	1341.8114	−33
1333.7869	2	1340.6688	20	1341.6686	−36	1341.8154	−52
1333.8434	35	1340.6728	−5	1341.6726	−39	1341.8195	−53
1333.8482	40	1340.6769	3	1341.6767	14	1341.8235	−52
1338.7317	−62	1340.6899	−28	1341.6807	22	1341.8302	−19
1338.7957	9	1340.6940	−28	1341.6953	2	1341.8343	14
1338.8479	8	1340.6980	−28	1341.6994	−9	1341.8383	19
1339.7590	13	1340.7021	−54	1341.7034	−14	1341.8424	42
1339.7666	4	1340.7061	−32	1341.7075	−59	1341.8464	−1
1339.7707	34	1340.7102	−16	1341.7115	−41	1341.8505	19
1339.7748	12	1340.7143	6	1341.7156	−43	1341.8545	−3
1339.7788	−17	1340.7183	−7	1341.7196	−22	1341.8586	−32
1339.7829	−19	1340.7963	−67	1341.7598	−80	1341.8627	−34
1339.8452	−70	1340.8004	−76	1341.7639	−40	1341.8667	−60
1339.8512	−53	1340.8044	−76	1341.7679	−82	1341.8708	−28
1339.8552	−43	1340.8085	−58	1341.7720	−39	1341.8748	−57
1339.8593	−21	1340.8125	−46	1341.7760	−24	1341.8789	−27
1339.8633	−22	1340.8166	−18	1341.7801	1	1341.8829	−37

[a]Heliocentric JD of mid-integration minus 2450000.

Table 3
Fits to Radial Velocities

Star	T_0[a]	P (d)	K (km s^{-1})	γ (km s^{-1})	σ (km s^{-1})
GW Lib	1340.6580 ± 0.0007	0.05332 ± 0.00002	38 ± 3	-17 ± 2	16
V844 Her	631.6119 ± 0.0010	0.054643 ± 0.000007	97 ± 11	-38 ± 8	47

[a]Apparent emission-line inferior conjunction, HJD −2450000.

TABLE 4
PHOTOMETRY LOG (V844 HER)

UT Date (1997)	Start[a]	Duration (h)	N_{points}	Tel.[b]	$\langle V \rangle$ (mag)	$T_{\max}$[c]	Amplitude (mag)
May 24	592.4162	4.10	243	1	13.09	592.4604	0.18
May 25	593.4381	2.55	75	2	13.17	593.4637	0.14
May 26	594.3971	4.97	250	1	13.27	594.4130	0.11
May 28	596.5536	10.43	773	3,4	13.54	596.5984	0.067
May 29	597.6080	5.90	375	3	13.62	597.6625	0.036
May 30	598.7468	5.61	222	4		598.7860	0.062
May 31	599.4120	13.72	870	1,2,4,5	13.70	599.4570	0.12
Jun 1	600.4180	12.97	716	2,3,4	13.72	600.4600	0.09
Jun 2	601.7096	6.68	348	4	13.90	601.7446	0.064
Jun 3	602.6403	7.68	400	4	14.04	602.6921	0.058
Jun 4	603.6619	7.12	213	5	15.2-15.7	603.6970	0.062
Jun 5	604.6566	7.44	471	4,5	17.00		< 0.05
Jun 10	609.6602	6.92	189	4	17.46	609.6672	0.18
Jun 11	610.6594	7.71	214	4	17.51	610.6734	0.23
Jun 14	613.6465	7.13	190	4	17.72	613.6678	0.15
Jun 15	614.6075	8.28	376	3,4	17.68	614.6769	0.22
Jun 16	615.6546	7.10	182	4	17.77	615.6703	0.16
Jun 17	616.6607	7.17	200	4	18.00	616.6729	0.16
Jun 20	619.5792	4.97	266	3	18.10	619.6075	0.16
Jun 28	627.5614	5.12	307	3	17.41		< 0.04
Jun 30	629.5679	2.12	114	3	17.28		

[a]Heliocentric JD of start, minus 2450000.

[b]Telescope codes: 1 = CBA-Belgium (25 cm); 2 = CBA-Denmark (25 cm); 3 = CBA-Maryland (66 cm); 4 = CBA-Tucson (35 cm); 5 = CBA-Braeside (41 cm).

[c]Heliocentric JD of superhump maximum, minus 2450000.

TABLE 5
SHORT-PERIOD DWARF NOVAE

Star	P_{orb} (d)	P_{sh}[a] (d)	ϵ	Source
V485 Cen	0.040995(1)	0.04216(2)	0.0284(5)	Augustein et al. (1996) Olech (1997)
RX2329+06	0.0445671(2)	0.0462(1)	0.037(3)	Thorstensen et al. (2002) Skillman et al. (2002)
GW Lib	0.05332(2)	···	···	This work
RX2353−38	0.0543234(?)	···	···	Augusteijn & Wisotzki (1997); Abbot et al. (1997)
DI UMa	0.054564(2)	0.05529(3)	0.0133(5)	Kato, Nogami, & Baba (1996); Fried et al. (1999)
V844 Her	0.054643(7)	0.05597(5)	0.0243(9)	This work
V592 Her	···	0.05653(13)	···	Duerbeck & Mennickent (1998)

[a] Superhump periods are slightly unstable. We adopt the mean value, or in the case of sparse data, an estimate 4 d after superhump onset. This reproduced the mean value for stars where both quantities could be observed. The estimated error in P_{sh} the error in estimating this quantity, not the full range of variation in P_{sh} (which is considerably larger).

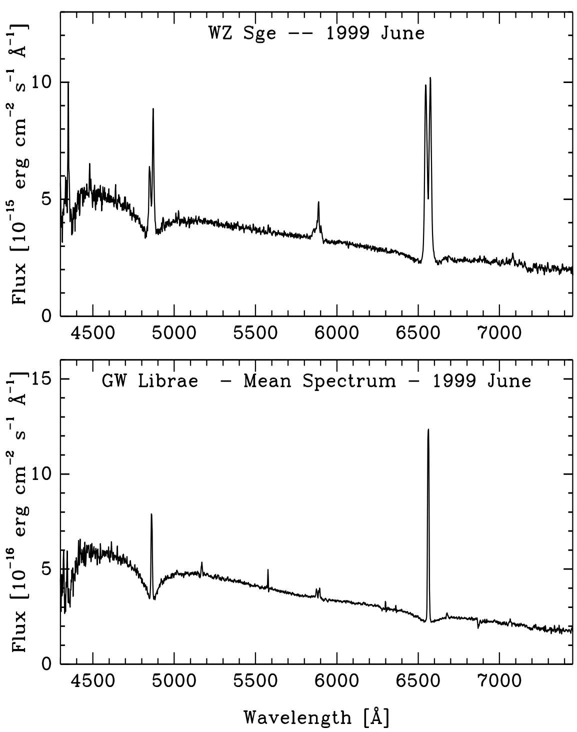

Fig. 1.— *Lower panel:* Mean spectrum of GW Lib. *Upper panel:* Spectrum of WZ Sge obtained for comparison. Note the similar broad Balmer absorption profiles from the white dwarf, and the markedly sharper emission lines in GW Lib.

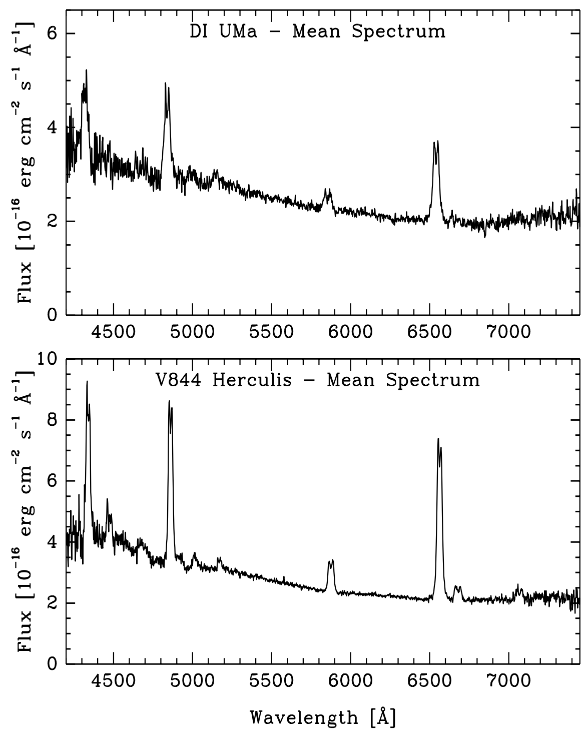

Fig. 2.— *Lower panel:* Mean spectrum of V844 Her. *Upper panel:* Mean spectrum of DI UMa, based on 19 6-minute exposures obtained 1997 Dec 17.510 - 17.556 UT.

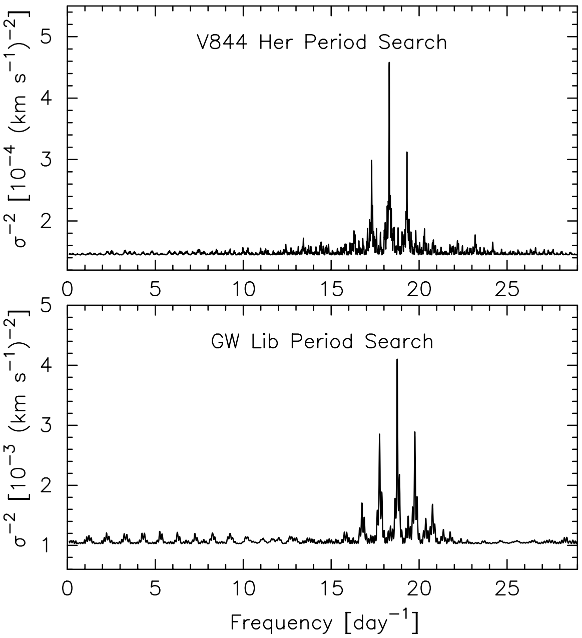

Fig. 3.— *Lower panel:* Period search 'residualgram' of the GW Lib Hα emission velocities. *Upper panel:* Period search of the V844 Her Hα emission velocities.

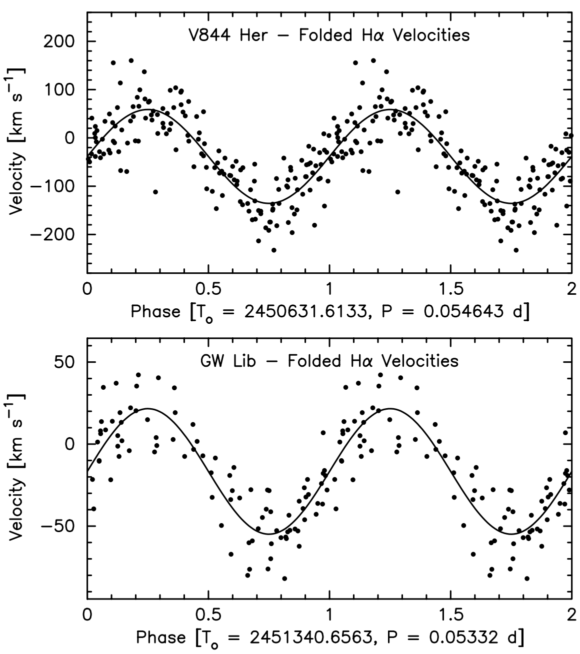

Fig. 4.— Hα velocities of GW Lib and V844 Her folded on the adopted periods, with best-fitting sinusoids superposed. All data are plotted twice to maintain continuity.

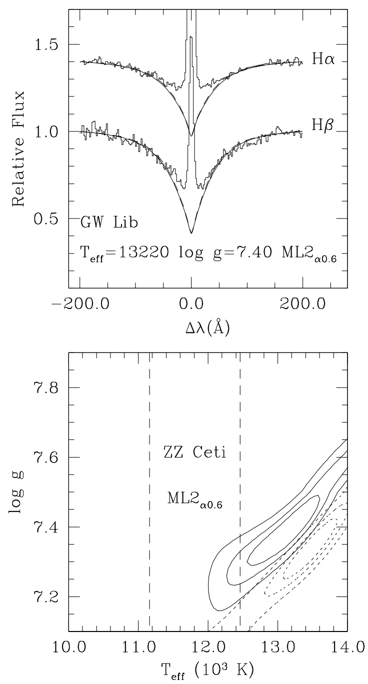

Fig. 5.— *Upper:* H α and Hβ profiles, with the best-fitting model atmosphere calculations superposed. *Lower:* contours of equal χ^2 on the $\log g$-$T_{\rm eff}$ plane. For the solid contours, a ± 50 Å interval around the line cores was excluded; the best fit is at $(T_{\rm eff}, \log g) = (13220 \text{ kelvin}, 7.4)$. For the dashed contours, ± 40 and ± 30 Å intervals were excluded at Hα and Hβ respectively, and the best fit is at $(13460 \text{ kelvin}, 7.34)$.

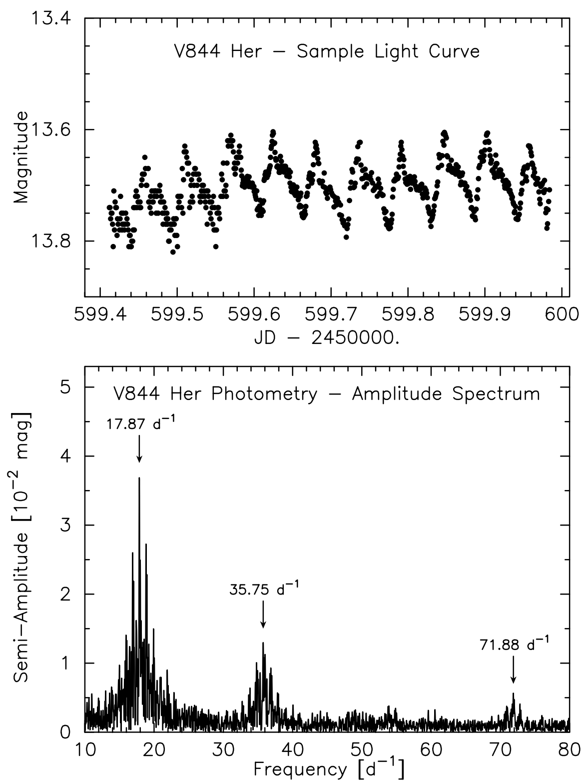

Fig. 6.— *Upper panel:* Superhumps observed in V844 Her on a single long night of photometric observation. *Lower panel:* Amplitude spectrum of 10 days of outburst photometry. The frequencies noted in the text are indicated with arrows.

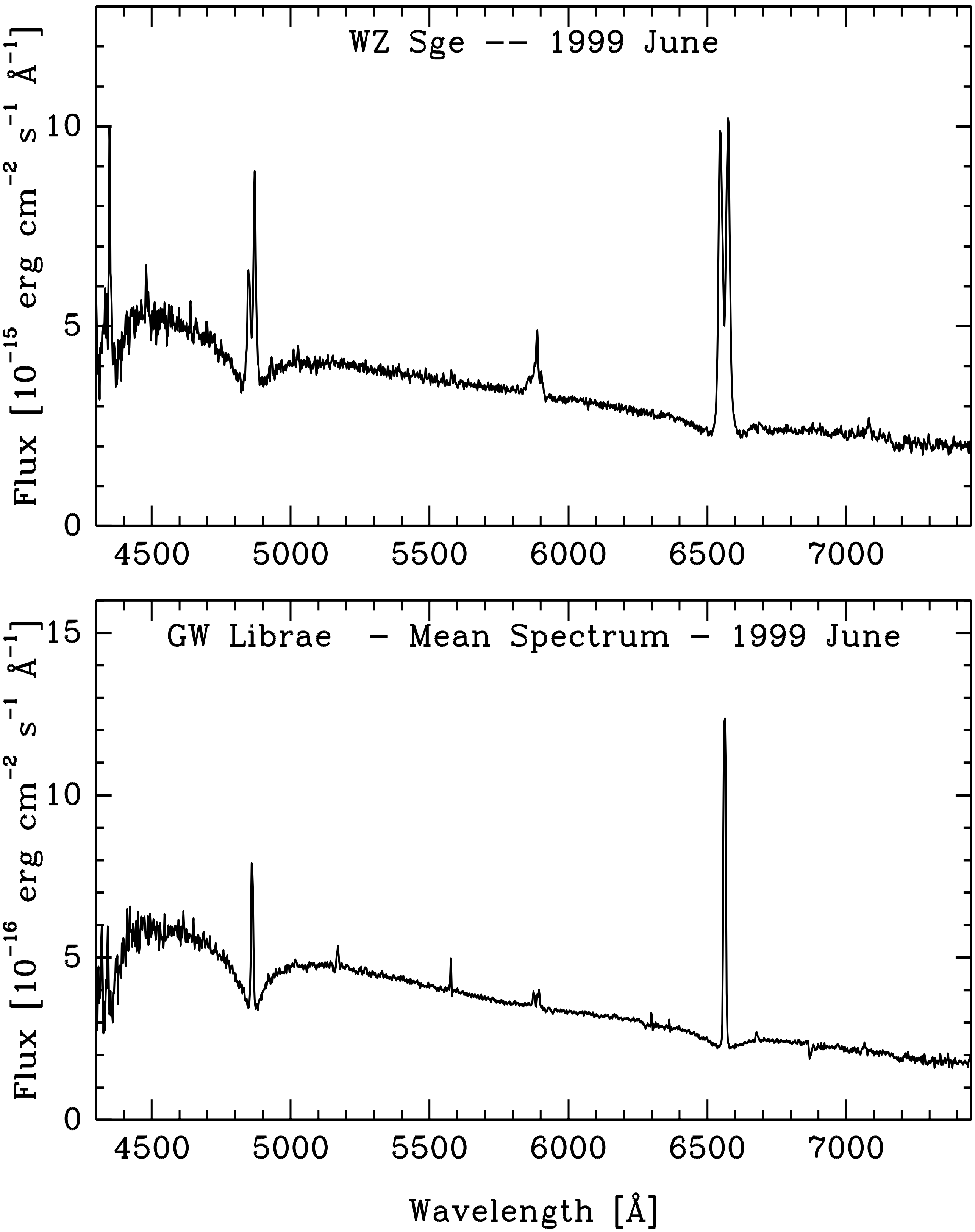
WZ Sge -- 1999 June
Flux [10^{-15} erg cm^{-2} s^{-1} Å^{-1}]
GW Librae - Mean Spectrum - 1999 June
Flux [10^{-16} erg cm^{-2} s^{-1} Å^{-1}]
Wavelength [Å]
4500
5000
5500
6000
6500
7000
0
5
10
15

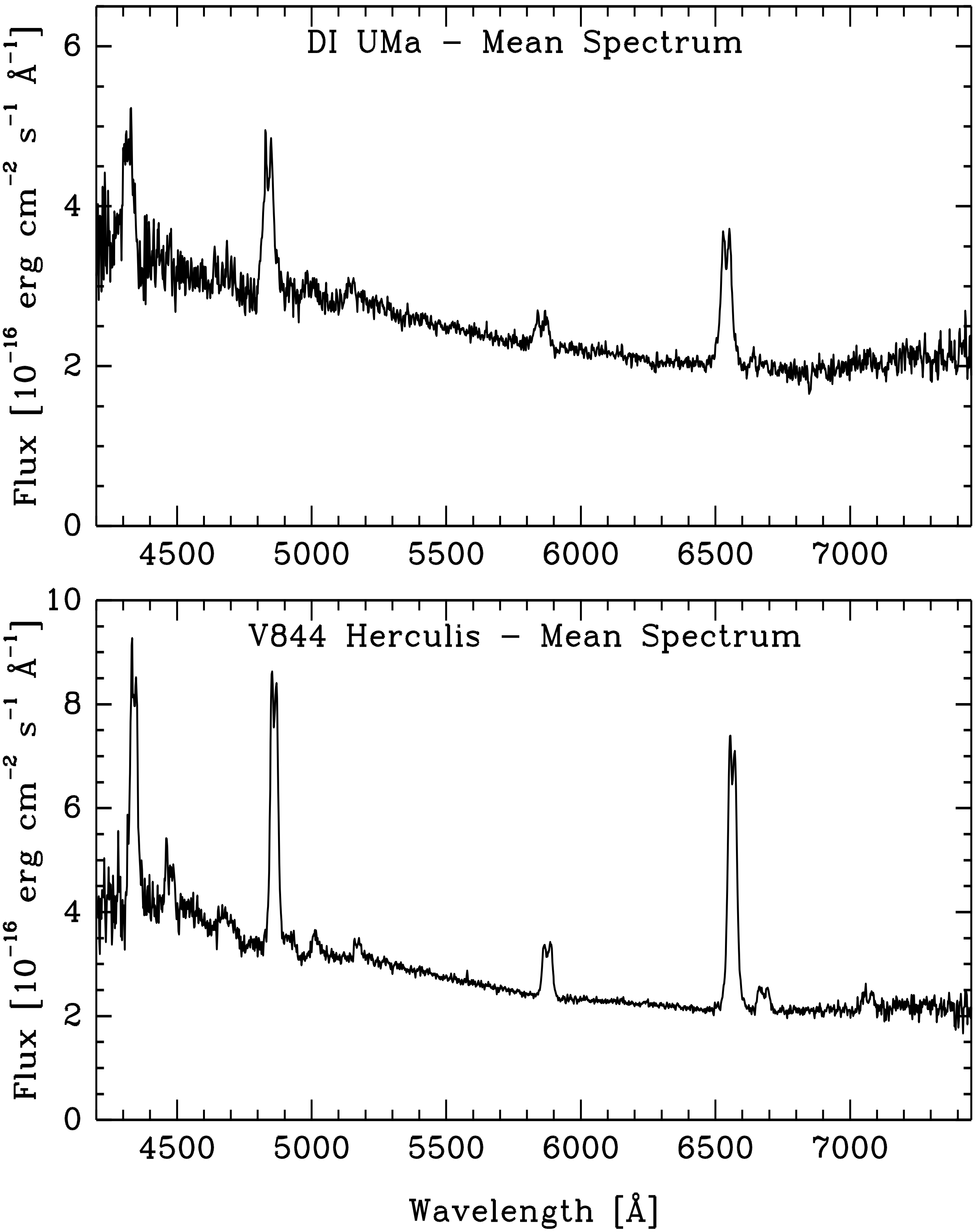
DI UMa - Mean Spectrum
Flux [10^{-16} erg cm^{-2} s^{-1} Å^{-1}]
0
2
4
6
4500
5000
5500
6000
6500
7000
V844 Herculis - Mean Spectrum
Flux [10^{-16} erg cm^{-2} s^{-1} Å^{-1}]
0
2
4
6
8
10
4500
5000
5500
6000
6500
7000
Wavelength [Å]